NISS

Variability of Travel Times on Arterial Links: Effects of Signals and Volume

Todd L. Graves, Alan F. Karr,
and Piyushimita Thakuriah

Technical Report Number 86
August, 1998

National Institute of Statistical Sciences
19 T. W. Alexander Drive
PO Box 14006
Research Triangle Park, NC 27709-4006
www.niss.org

Variability of Travel Times on Arterial Links: Effects of Signals and Volume

Todd L. Graves*
National Institute of Statistical Sciences and Bell Laboratories
Alan F. Karr
National Institute of Statistical Sciences
Piyushimita Thakuriah
National Institute of Statistical Sciences and University of Illinois at Chicago

Abstract

We use detailed probe, video and detector data to characterize variability of travel times on (one link of) a major arterial street in the Northwest suburbs of Chicago. Major influences on variability are shown to be signal status and traffic volume, vehicles' entry times of the link relative to the start of a red phase at the downstream intersection and the numbers of cars queued when they arrive at that signal. Because these primary determinants of travel time are not accessible in many situations, we show how to predict them from others that are more readily available.

1 Introduction

Understanding variability of vehicle travel times is central to understanding traffic flow on arterial streets. This paper uses detailed data from probes, video and detectors to explain the variability of travel times on a signalized arterial in Northwest suburban Chicago. Specifically, using models described in §3, a vehicle's travel time is shown to be determined with high accuracy by the timing of its entry onto a link relative to the downstream traffic signal and number of other vehicles queued in front of it when it reaches that signal. Our approach is similar in spirit to Petty, *et al.* (1998), which treats accurate estimation of freeway travel times.

Prediction of travel times is plausibly the most likely application of the models in §3. Characterization of variability is an essential component in prediction, for example, to provide dynamic route guidance in an advanced traveler information system (ATIS). While the methods in this paper in no sense constitute an ATIS, we do discuss in §4 how they can be adapted for predictive

*Research supported by National Science Foundation grants DMS-9208758 and DMS-9313013 to NISS.

purposes. The principal issue is that the determinants of variability identified in §3 are not readily available (that is, are not measured) in most settings, so in §4 we show how to predict them from other variables that are more likely to be available.

2 Data

Three forms of data are used in this paper: travel times collected by probe vehicles (§2.1); signal status and vehicle exit times obtained from video cameras (§2.2); and volumes recorded by loop detectors (§2.3).

Data were collected, as described in Sen, *et al.* (1997), from a small subnetwork of the ADVANCE project (Boyce, *et al.*, 1994) network, consisting of Dundee Road (in North suburban Chicago) between Wheeling Road and Elmhurst Road, and adjacent links.

Analysis focused on one *study link*: the 427-meter link of Westbound Dundee Road from Wheeling Road to Elmhurst Road. It consists of two lanes and can be entered and exited by a through movement or either a left turn from a dedicated lane or right turn. The speed limit is 35 MPH; travel times vary from less than 30 seconds to more than 100.

The link is signalized at both intersections. At the downstream intersection, an arrow at the start of each green phase allows protected left turns; left turns are also allowed during the primary green phase itself. The signal cycle is approximately 130 seconds, split evenly between green and red.[1] Phase lengths may be prolonged on the basis of detector data.

2.1 Probe Data

Probe vehicles from the ADVANCE project provided time-stamped travel times along each link traversed. The time stamp is, for practical purposes, the time at which the vehicle exits the link.

The probes were driven by non-professional drivers. To avoid confounding drivers with other effects, routes were Markov chains constructed by randomizing over turns at each intersection, using weights that give preference to the study link. Data were collected from 27 probes traveling between 1:00 PM and 8:00 PM on 25 days during the period July 5 – August 19, 1995. A total of 3986 travel times were recorded for the study link.

2.2 Video Data

Video data were collected between 3:00 PM and 6:00 PM in late July and early August, 1995, for a total of 10 days, concurrent with ADVANCE evaluation tests (Argonne, 1997). Two video cameras were placed at the downstream intersection. One, at the Northwest corner, filmed *all* cars exiting the link. The second, at the Southeast corner, recorded the traffic signal at the end of the link. The time stamps on the cameras were synchronized to the ADVANCE system clock.

Extracted from the video tapes, using simple, NISS–developed software, were: (1) The time-dependent status of the downstream signal of the study link; (2) Exit times from the study link, by

[1] For simplicity, we absorb the amber phase into the green.

turning movement, of *all* vehicles; and (3) Exit times, by turning movement and vehicle ID, for probes.[2] From these data were derived the number of vehicles that exited the link during the same green phase as a probe, the probe's rank among these vehicles and the status of the signal at and after the probe's entry of the link.

2.3 Detector Data

Single-loop detectors are located in each lane of Dundee Road some three hundred feet upstream (East) of the Dundee–Elmhurst intersection. The data, aggregated to five-minute intervals, comprise both counts and occupancies; those relevant to a probe's travel time are the measurements for the five-minute interval containing the entry time. As observed elsewhere, quality is a serious problem for detector data.[3]

3 Models that Explain Variability

In this section, we use simple models to show that selected characteristics of the traffic signals and volume account for much of the variability in probe travel times on the study link. The models are quite similar to delay functions used in a variety of applications (e.g., network flow models).

3.1 Through Exits

We first discuss cars that exit the study link using a through movement.

One critical variable in explaining variability of travel times is *relative entry time* — the time RET that the probe enters the link relative to the status of the downstream signal. A vehicle has RET $= t$ if, were it to drive to the end of the link at the free flow speed, it would arrive there t seconds after the exit signal changed to red. Figure 1 shows a scatter plot of travel time TT and relative entry time RET for probe vehicles exiting via a through movement.

Figure 2 presents a model for these data in terms of RET and traffic volume.[4] Suppose that the traffic volume is v (vehicles per second) and that each vehicle requires c seconds to clear the queue (see (3) below), and assume that $cv < 1$ and that $cvR < G$.[5] Thus, when RET $< R/(1-cv)$, a vehicle must wait in a queue at the end of the link, adding a queueing delay to its travel time. The resulting model is

$$\text{TT(RET)} = \begin{cases} \text{FFTT} + R - (1-cv)\text{RET} & \text{RET} \le R/(1-cv) \\ \text{FFTT} & R/(1-cv) < \text{RET} \le R+G, \end{cases} \qquad (1)$$

[2] Probes carried markers that allowed them to be identified in the video data.

[3] In Graves, *et al.* (1998a), more than 40% of detector measurements were palpably flawed; the true error rate is even higher.

[4] Assumptions implicit in this model are that signal behavior is nonrandom and that acceleration between rest and the free flow speed is instantaneous.

[5] Otherwise the system is unstable.

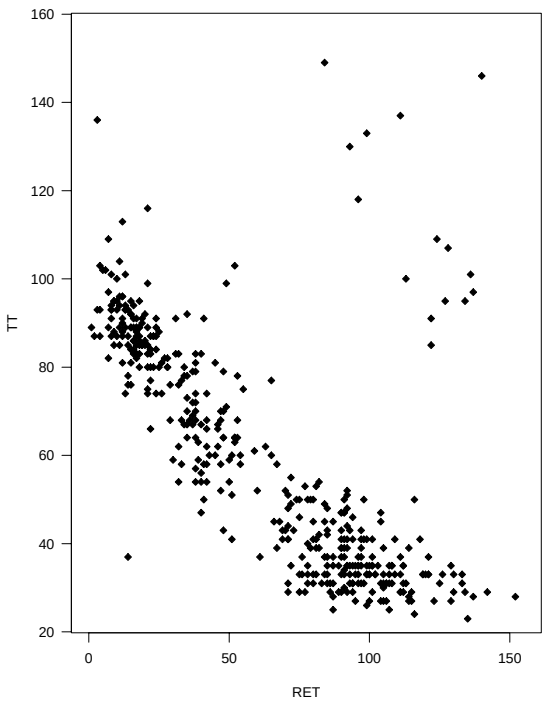

Figure 1: Data for Through Exits: Probe Travel Times vs. Relative Entry Times.

where FFTT is the free flow travel time.[6]

Neither (1) nor (2) below represents explicitly the cruise time of vehicles: delays along the link are presumed compensated by a shorter wait at the link's end.

Because video data are available, we re-parameterize (1) to model TT as a function of RET and POS — one plus the number of vehicles exiting the intersection in the same green cycle but prior to the vehicle under consideration:

$$\mathrm{TT}(\mathrm{RET}, \mathrm{POS}) = \mathrm{FFTT} + [\mathrm{TC}(\mathrm{POS}) - (\mathrm{RET} - R)]_+ , \tag{2}$$

where $\mathrm{TC}(n)$ is the time required for a queue of n vehicles to clear.

The model (2) was fitted as follows. First, FFTT $=$ 27 seconds, obtained by dividing the link length by the speed limit. Second, using vehicle exit times from video data and the `rreg()` procedure in *S-Plus* with Huber weights (Venables & Ripley, 1994), the function TC is estimated to be

$$\mathrm{TC}(n) = 3.5 + 1.2n. \tag{3}$$

[6] An idealized form arises when $v = 0$: $\mathrm{TT}(\mathrm{RET}) = \mathrm{FFTT} + (R - \mathrm{RET})_+$, where x_+ is equal to x if $x \geq 0$ and $x_+ = 0$ otherwise.

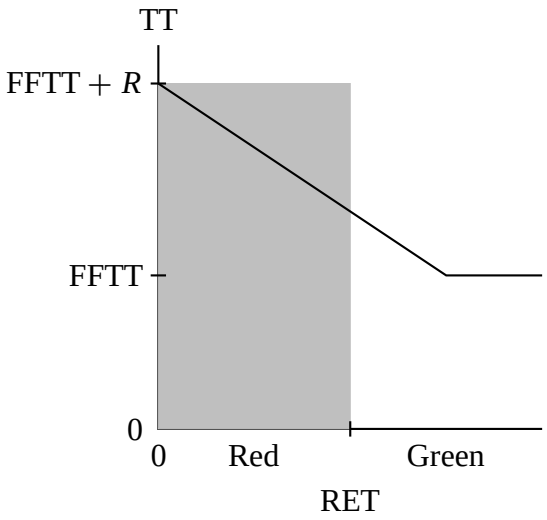

Figure 2: Model (1) for Travel Time (TT) as a Function of Relative Entry Time (RET). FFTT is the free flow travel time. The signal is red during the shaded times.

(This model differs from the queue-clearing model embedded in (1) by the presence of the constant term 3.5; 1.2 corresponds directly to c in (1).) The fitted version of (2) is then

$$\text{TT}(\text{RET}, \text{POS}) = 27 + [3.5 + 1.2 \times \text{POS} - (\text{RET} - R)]_+ ; \tag{4}$$

R is approximately 60 seconds.

Figure 3 plots probe travel times against fitted values from (4). The fit is very good: the median absolute residual is two seconds, and only thirty out of 426 probes have residuals greater than eight seconds in absolute value.[7] Most cases where the fit is poor constitute *cycle failures*: vehicles that, based on RET, should have arrived at the signal while it was still green, but did not. Several probes met this fate, as seen in Figure 1.

Therefore, RET, POS and R explain essentially completely the variability in TT.

3.2 Right Exits

Travel times of probes that exit the study link by turning right behave substantially the same as for through exits.

Figure 4 (left) shows the data: probe travel times plotted against relative entry times. Corresponding to (4) is the model

$$\text{TT}(\text{RET}, \text{POS}) = 27 + \left[2.4 + 1.1 \times \text{POS}^* - (\text{RET} - R)\right]_+ , \tag{5}$$

[7] The line added, for clarity, to this graph is the forty-five degree line, as will be the case with analogous graphs below.

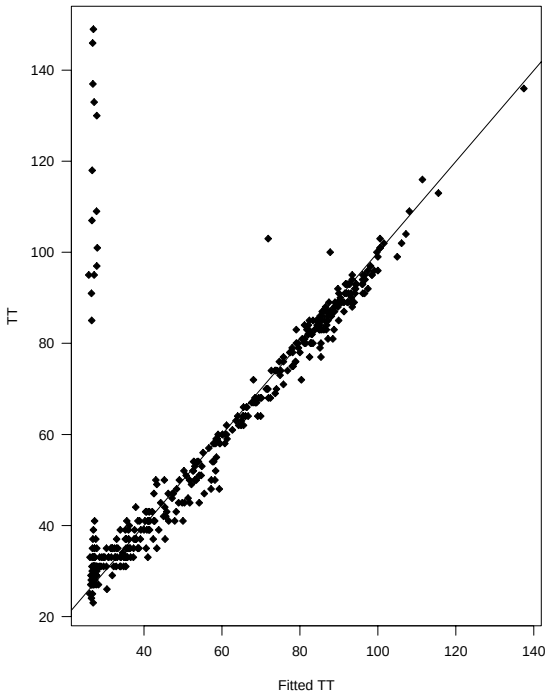

Figure 3: Results for Through Exits: travel times vs. fitted values from (4).

where POS* is equal to one plus the number of cars that exit before the probe by a right or through movement. Figure 4 (right) plots probe travel times against fitted values from (5).

Decrease in the coefficients relative to the through movement data may result from our ignoring the right-turning traffic in the analysis of the probes that take through exits, or from lane differences, since all right-turning probes exit in the right lane. The plot differs from Figure 3 in that several probes had low travel times that the model predicts to be high; these were probably able to turn on red.

3.3 Left Exits

The situation for probes that exit the study link by turning left is more complicated. Three travel time patterns arise, as visible in the upper left panel of Figure 5:

1. A vehicle can exit during the *protected left* signal during the same cycle that it arrived at the end of the link. Because the protected left signal is at the start of the green phase, such vehicles will have shorter travel times than had they gone straight instead.

2. A vehicle can exit during the same cycle via an *unprotected left*. Doing so requires waiting for the opposing traffic to clear, leading to moderate travel times.

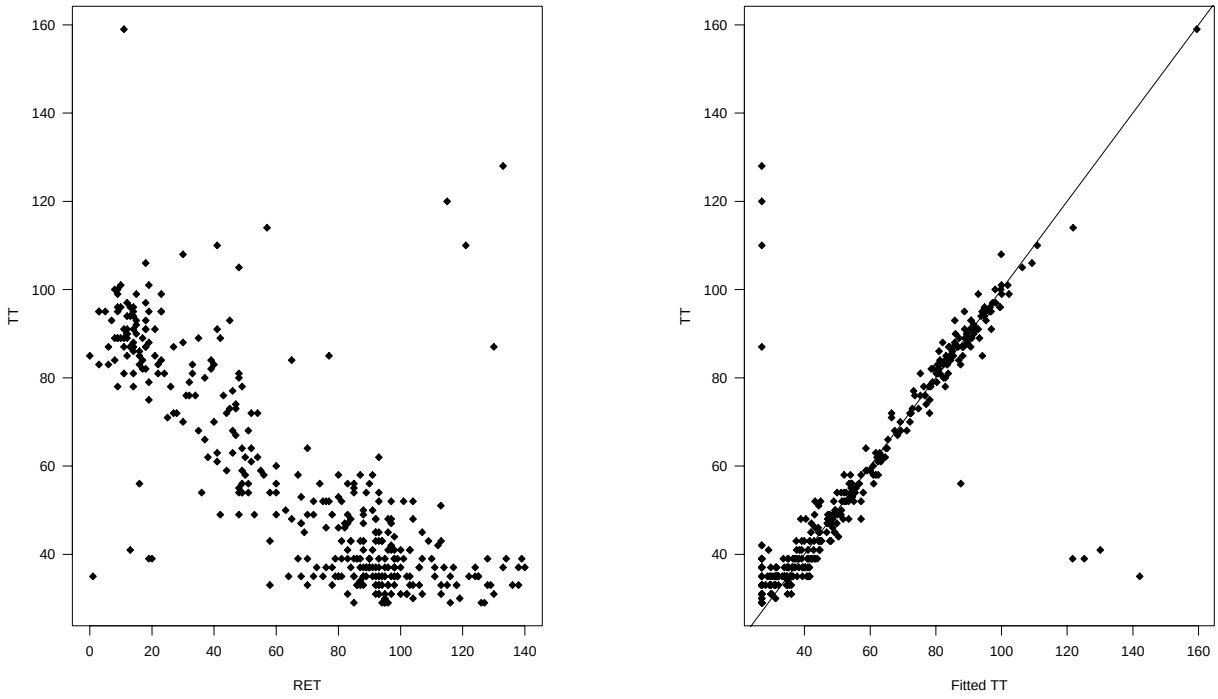

Figure 4: Right Exits. *Data (left):* Probe travel times vs. relative entry times. *Results (right):* Probe travel times vs. fitted values from (5).

3. A vehicle can experience a *cycle failure* if opposing traffic never thins sufficiently to allow turning across its lanes. In our data, all such vehicles were able to turn during the protected left of the next cycle; obviously they have long travel times.

The analysis for the protected group is as for through and right exits, resulting in the model

$$\mathrm{TT}(\mathrm{RET}, \mathrm{POS}) = 27 + \left[3.1 + 2.0 \times \mathrm{POS} - (\mathrm{RET} - R^*)\right]_+, \tag{6}$$

where $R^* \approx 51$ seconds is the time the light is red before turning to a left arrow. Figure 5 (upper right) plots probe data against fitted values from (6). The regression coefficients differ from those for through and right exits because only one lane turns left.

To treat the unprotected left group, which has the greatest variability, we introduce additional variables. Let LAS and LAE be the start and end times for the left arrow signal in the cycle that the probe exits. Let OQS be the time at which the opposing queue begins to move (typically, OQS $=$ LAE), and let OQC be the time necessary for the opposing traffic (traveling East on Dundee Road) to clear, at which point unprotected left turns can begin. For simplicity, we assume that no opposing traffic arrives after OQC, so that no further waiting is necessary.[8]

[8]To the extent that this is not true, discrepancies will be reflected in regression coefficients.

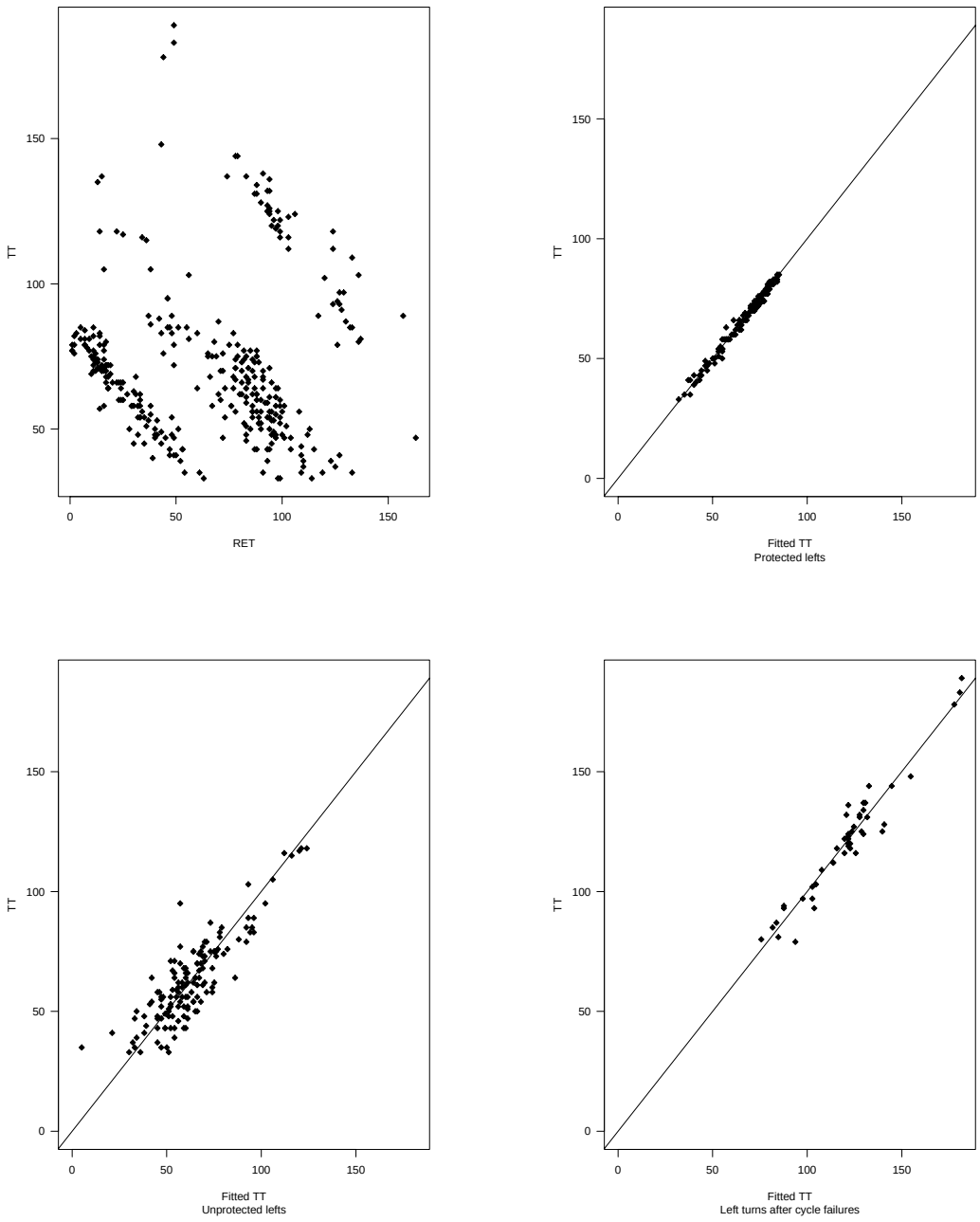

Figure 5: Left Exits. *Upper Left:* Data — probe travel times vs. relative entry times. *Upper Right* Results for protected left subset — travel times vs. fitted values from (6). *Lower Left* Results for unprotected left subset — travel time vs. fitted values from (7). *Lower Right* Results for cycle failure subset — travel time vs. fitted values from (8).

Using the queue-clearing model (3) with the parameters from (6) leads to the model

$$\mathrm{TT}(\mathrm{RET}, \mathrm{POS}) = \mathrm{OQS} - \mathrm{RET} + \mathrm{OQC} + 6.2 + 2.0 \times \mathrm{POS} - (\mathrm{LAE} - \mathrm{LAS}). \tag{7}$$

Probe travel times are plotted against fitted values from (7) in the lower left panel of Figure 5. There we have taken $\mathrm{OQC} = 48$ seconds, which produced the best fit. None of our data were useful to estimating the value of OQC. Detector data from the opposing link might be valuable, although both quality and the too-coarse five minute aggregation militate against their use.

By analogy with (6), a model for vehicles undergoing cycle failure is

$$\mathrm{TT}(\mathrm{RET}, \mathrm{POS}) = 27 + \left[3.1 + 2.0\mathrm{POS}^* - (\mathrm{RET} - R^*)\right]_+, \tag{8}$$

where POS^* is the vehicle's position in the queue after left turns on its entry cycle are completed. This can be estimated from its original position, the length $(\mathrm{LAE} - \mathrm{LAS})$ of the green arrow and a value (estimated from the data to be 3.25) for the number of cars that take unprotected left turns during the cycle before the probe's exit cycle. Data are plotted against fitted values from (8) in the bottom right panel of Figure 5.

4 Predicting Travel Times

The models §3 explain variability by representing travel times as functions of RET, POS, R, and, for vehicles turning left, the group to which they belong. In many settings, as noted in §1, these may either not be available or not be known in advance.[9] In this section, we show how to predict RET and POS from other, more readily accessible observations. Except in §4.4, we consider only vehicles exiting the study link via through movements.

The approach is straightforward: replace key variables in (4) (and corresponding equations for other exit movements) by predicted values, continuing to use the estimated values of the parameters. For (4), this leads to the prediction equation

$$\widehat{\mathrm{TT}} = 27 + \left[3.5 + 1.2 \times \widehat{\mathrm{POS}} - (\widehat{\mathrm{RET}} - \widehat{R})\right]_+, \tag{9}$$

where the carets denote predicted variables. Some properties of this equation are discussed in §4.4. The issue, at this point, becomes calculation of the predicted values on the right-hand side of (9).

4.1 Predicting RET

The distribution of relative entry time as a function of the entry movement has significant predictive power, illustrated by the histograms in Figure 6, where rows correspond to *entry* movements left, right and through. The two columns in Figure 6 are before and after 4:00 PM, a time at which signal settings are changed.

[9] The latter case arises in predicting future link travel times for an ATIS.

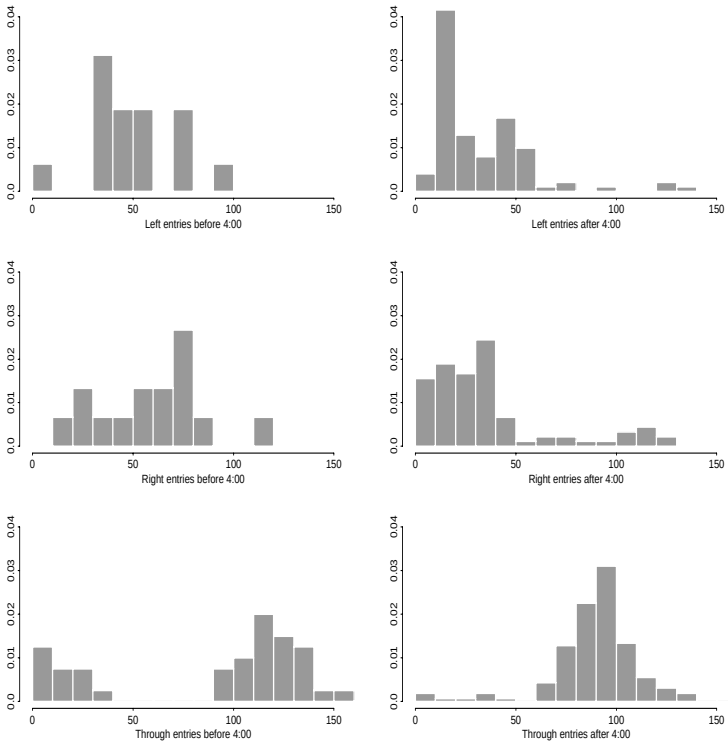

Figure 6: Histograms of Relative Entry Times by Entry Movement and Time of Day. *Top:* Entry via left turn. *Middle:* Entry via right turn. *Bottom:* Through entry. *Left:* prior to 4:00 PM. *Right:* After 4:00 PM.

There are clear differences among the distributions, which are especially pronounced after 4:00 PM. These are due to signal synchronization, which favors through traffic on Dundee Road (a major arterial).

The means of the distributions in Figure 6 constitute predictors $\widehat{\text{RET}}$ — for use in (9) — that are functions of time of day and entry movement.

4.2 Predicting R

Figure 7 contains kernel density estimates (smoothed histograms) of the distribution of R before and after 4:00 PM. The associated means become the predictors $\widehat{R}$ in (9).

4.3 Predicting POS

Rather than predict POS directly, we predict NV, the number of cars that exit via a through movement during the same cycle as the probe. Clearly POS lies between 1 and NV, with large values corresponding to large relative entry times. If arrivals at the end of the link were uniform over a

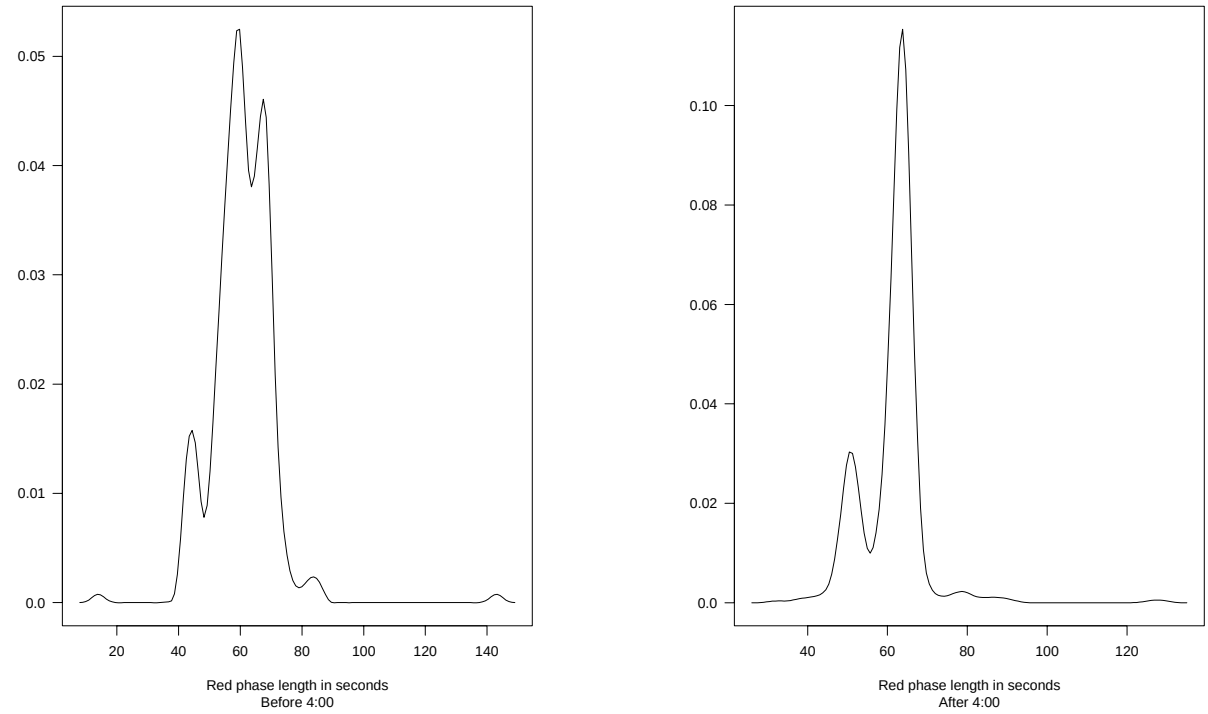

Figure 7: Kernel Density Estimates of Red Phase Length by Time of Day. Left: Prior to 4:00 PM. *Right:* After 4:00 PM.

signal cycle, we would have

$$\text{POS} = \frac{\text{RET}}{R+G}\,\text{NV}. \tag{10}$$

One model leading to (10) assumes that arrivals at the end of the link follow a Poisson process whose intensity parameter reflects the volume of traffic, which can estimated as a function of time of day from detector counts.[10]

Figure 8 contains plots of POS/NV against RET, before (left) and after (right) 4:00 PM.[11] Arrivals are relatively homogeneous before 4:00, which is evidence in support of (10), but less so afterward. The second plot suggests a piecewise linear fit, which could be interpreted as one arrival rate while the exit light is red and a larger arrival rate while the exit light is green; (10) could then be modified correspondingly.

From (10), given a predictor $\widehat{\text{NV}}$, we can predict POS directly:

$$\widehat{\text{POS}} = \frac{\widehat{\text{RET}}}{\widehat{R+G}}\,\widehat{\text{NV}}, \tag{11}$$

[10] This is an approximation: since cars travel in platoons, the observed data are over-dispersed relative to the Poisson model.

[11] Adjustment for cycle failures is described in §3.3.

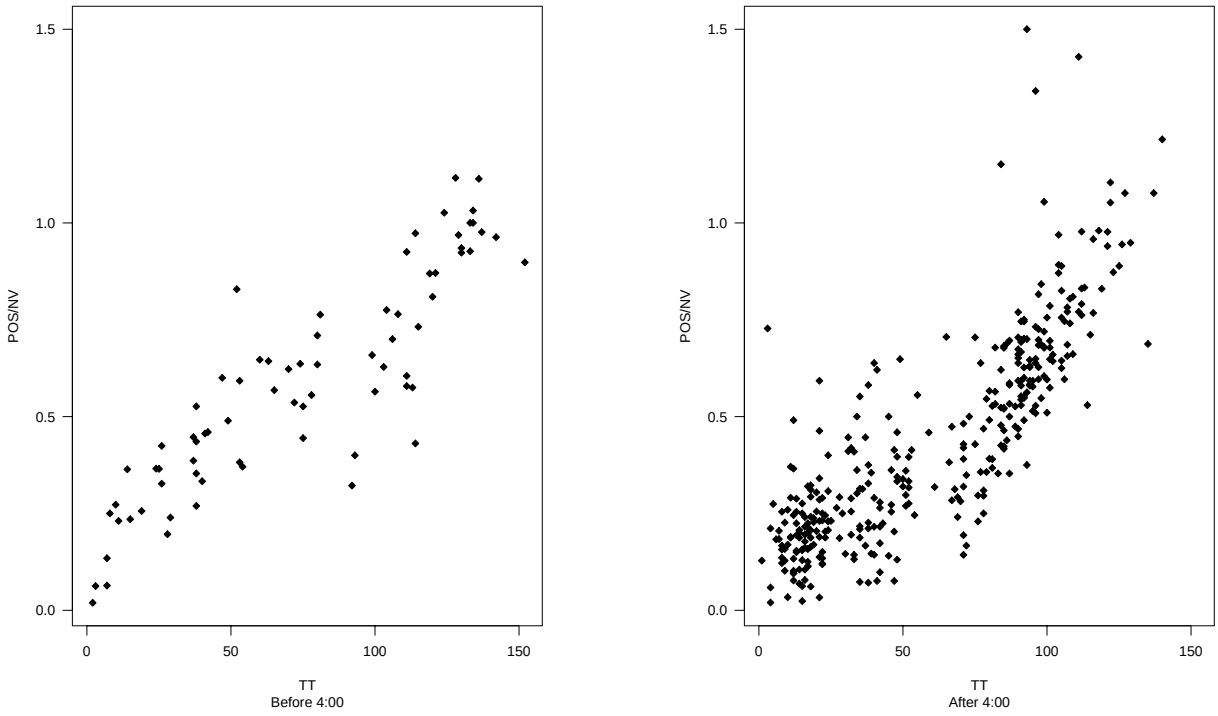

Figure 8: Position in queue relative to queue length as a function of relative entry time. *Left:* Before 4:00 PM. *Right:* After 4:00 PM.

where $\widehat{\text{RET}}$ and $\widehat{R}$ are calculated as in §4.1 and 4.2.[12]

Finally, NV can be predicted using detector data. Figure 9 plots exit counts per signal cycle (from video data) — that is, NV — against 5-minute detector counts. The visible, positive relationship, however, is not strong statistically because of over-aggregation and low quality of data from the detectors.[13]

4.4 Other Prediction Issues

Here we discuss two additional issues associated with prediction.

Predicting Left Turn Group. Modification of the methodology described at the beginning of the Section to apply to other turning movements is largely straightforward, except that for vehicles exiting via a left turn, it is necessary to predict to which of the three groups described in §3.3 they belong. Group membership is closely related to POS, as seen in Table 1. Each column corresponds to a value of POS and lists the numbers of probes with that value of POS that fall in each of the

[12] $\widehat{G}$ is calculated using distributions analogous to those in Figure 7, omitted here for brevity.

[13] An approximate calculation suggests that recorded counts are 18% too low.

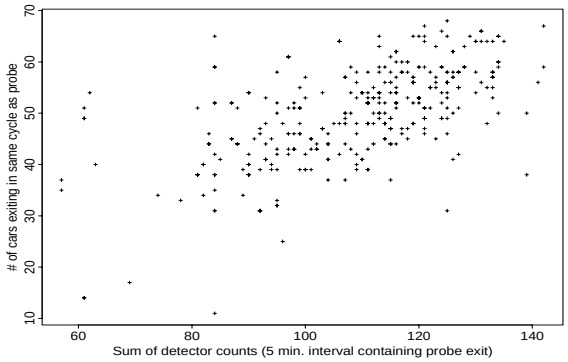

Figure 9: Video Exit Volumes (per signal cycle) vs. Five-Minute Detector Counts.

	1	2	3	4	5	6	7	8	9	10
Group 1:	13	27	23	19	15	5	9	5	1	0
Group 2:	1	9	11	12	19	20	21	19	14	14
Group 3:	1	0	0	0	0	1	1	5	2	8
	11	12	13	14	15	16	17	18	19	20
Group 1:	0	0	0	0	0	0	0	0	0	0
Group 2:	10	8	3	2	0	1	1	1	0	0
Group 3:	11	6	9	3	2	2	0	2	0	1

Table 1: Left Turn Group Membership as a Function of POS.

three groups: POS ≤ 4 tends to imply Group 1, while POS ≥ 13 suggests Group 3, the remainder going into Group 2.

Predicting Travel Time Distributions. Prediction of mean travel times is immediate: means of the distributions discussed in §4.1–4.3 can be inserted directly into (9).

In other settings, however, the entire *distribution* of travel times $\widehat{\text{TT}}$ in (9) may be of interest; for example, distributions are needed to combine travel time predictions for individual links to form a predicted travel time for a multi-link route. While (9) still applies, possible dependence among $\widehat{\text{RET}}$, $\widehat{\text{POS}}$ and $\widehat{R}$ must be addressed.

The fundamental ingredients of (9) are $\widehat{\text{RET}}$, which is derived from probe data (see Figure 6), $\widehat{R}$ and $\widehat{G}$, derived from video data, and $\widehat{\text{NV}}$, which is derived from detector data. It is plausible to assume that $\widehat{\text{RET}}$, the pair $(\widehat{R}, \widehat{G})$ and $\widehat{\text{NV}}$ are conditionally independent given the time of day.[14] (For demand-actuated signals, this conditional independence is less plausible.) Clearly $\widehat{R}$ and $\widehat{G}$ are not independent, but a joint distribution can be derived from video data.

From these objects, the joint distribution of $(\widehat{\text{RET}}, \widehat{R}, \widehat{G}, \widehat{\text{NV}})$ can be derived, which coupled with (10) yields that for $(\widehat{\text{RET}}, \widehat{\text{POS}}, \widehat{R})$. The latter, via (9), then yields the distribution of $\widehat{\text{TT}}$.

[14] Application of (9) yields time-of-day-dependent predictions.

5 Conclusions

The models presented here apply to travel times for moderate traffic on arterial streets. They are not strongly location-dependent, but may not apply if our assumption that cruise delays are compensated by shorter queueing delays fails, which occurs, for example, in highly congested settings characterized by frequent, possibly multiple cycle failures. Context-dependent parameters (e.g., free flow travel times, signal characteristics and volumes) would need to be observed or estimated. By contrast, the regression coefficients that parameterize queue clearing probably do not change radically from one setting to another. Qualitative differences (for example, absence of dedicated left turn lanes or complicated intersection geometries) would require more detailed consideration.

Acknowledgments

We thank the management of the ADVANCE project for making probe vehicles available for this study, Ashish Sen (UIC) for general advice, Daryl Daley (Australian National) for many discussions, Siim Sööt (UIC) for vital assistance during data collection, students from UIC who drove the probe vehicles, and a graduate student from UNC-CH who extracted data from the video tapes.

References

Evaluation Manager, Argonne National Labortory (1997). *The ADVANCE Project: Formal Evaluation of the Targeted Deployment*. Sponsored by the U.S. Department of Transportation, Federal Highway Administration, Joint Program Office. Three volumes.

Boyce, D. E., Kirson, A. M., and Schofer, J. L. (1994). ADVANCE — The Illinois navigation and route guidance demonstration program. In Catling, I., ed., *Advanced Technology for Road Transport*. Artech House, Boston.

Graves, T. L., Karr, A. F., Rouphail, N. M., and Thakuriah, P. (1998). Real-time prediction of incipient congestion on freeways from detector data. Submitted to *Transp. Sci.*

Petty, K., Bickel, P., Jiang, J., Ostland, M., Rice J., Ritov, Y., and Schoenberg, F. (1998). Accurate estimation of travel times from single-loop detectors. *Transp. Res. A* **32(1)** 1–17.

Sen, A., Thakuriah, P., Zhu, X. and Karr, A. F. (1997). Frequency of probe reports and variance of travel time estimates. *J. Transp. Engrg, ASCE* **123(4)**.

Thakuriah, P., Sen, A. and Karr, A. F. (1997). Probe-based surveillance for travel time information in ITS. *Behavioral and Network Impacts of Driver Information Systems*. Ashgate/Avebury, UK. (to appear)

Venables, W. N., and Ripley, B. D. (1994). *Modern Applied Statistics with S-Plus.* Springer, New York.